SCIENCE CHINA
Earth Sciences

•RESEARCH PAPER•

April 2021 Vol.64 No.4: 559–570
https://doi.org/10.1007/s11430-020-9711-2

# Evidence for glaciation predating MIS-6 in the eastern Nyainqêntanglha Range, southeastern Tibet

Shangzhe ZHOU[1], Jinming XIE[2], Xianjiao OU[3], Liubing XU[1*], Yong SUN[4], Xuezhen ZENG[4], Xiaoxia WEN[1], Renrong CHEN[3], Hong YANG[1], Xianmei HUANG[1], Yazhong ZHOU[1] & Jinjin SUN[1]

[1] *Department of Geography Science, South China Normal University, Guangzhou 510631, China;*
[2] *College of Earth and Environmental Sciences, Lanzhou University, Lanzhou 730000, China;*
[3] *School of Geography and Tourism, Jiaying University, Meizhou 514015, China;*
[4] *Key Laboratory of Tibetan Environment Changes and Land Surface Processes, Institute of Tibetan Plateau Research, Chinese Academy of Sciences, Beijing 100101, China*

Received June 3, 2020; revised September 12, 2020; accepted December 15, 2020; published online February 8, 2021

**Abstract** Southeastern Tibet is one of the most glaciated regions on the Tibetan Plateau both at present and during the Quaternary. Numerical dating of glacial deposits has allowed the establishment of a provisional chronology of Quaternary glacial fluctuations in this region, with the oldest glaciation (Guxiang Glaciation) occurring in marine oxygen isotope stage 6 (MIS-6). During our recent field investigations, a morphostratigraphically older lateral moraine than that of the Guxiang Glaciation has been first identified, which is ~500–600 m above the Guxiang Glaciation moraine and discontinuously preserved on valley shoulders in the Bodui Zangbo River valley, eastern Nyainqêntanglha Range in southeastern Tibet. Considering the moraine is best preserved at Nitong Village, here we name the glacier advance which deposited the moraine as "Nitong Glaciation". Using electron spin resonance (ESR) technique, we dated the Nitong Glaciation moraine to 506.3±60.4 ka. Taking into account the age error and climatic conditions, we consider it most likely that the Nitong Glaciation occurred during MIS-12, although it might had happened sometime earlier.

**Keywords** Southeastern Tibet, MIS-12 Glaciation, ESR dating, Quaternary Glaciation

**Citation:** Zhou S, Xie J, Ou X, Xu L, Sun Y, Zeng X, Wen X, Chen R, Yang H, Huang X, Zhou Y, Sun J. 2021. Evidence for glaciation predating MIS-6 in the eastern Nyainqêntanglha Range, southeastern Tibet. Science China Earth Sciences, 64(4): 559–570, https://doi.org/10.1007/s11430-020-9711-2

## 1 Introduction

Southeastern Tibet, adjacent to the eastern Himalayan syntaxis, is characterized by high-relief mountain ranges (eastern Nyainqêntanglha Range and eastern Himalaya Mountains) alternating with deeply-incised river valleys (Yarlung Zangbo River and its tributaries, like Bodui Zangbo, Parlung Zangbo, and Yigong Zangbo Rivers). These valleys are corridors through which moisture brought by the Indian summer monsoon flows into southeastern Tibet, resulting in the eastern Nyainqêntanglha being the region with the highest precipitation on the Tibetan Plateau. Facilitated by the high precipitation, the eastern Nyainqêntanglha is one of the most glaciated regions on the Tibetan Plateau both at present and during the Quaternary. So far, considerable attention has been paid to investigating and dating glacial sequences in this region. For example, in the 1970s, Li et al. (1986) found evidence for two major phases glacier advances in the Bodui Zangbo River valley in the eastern Nyainqêntanglha and named them as Guxiang and Baiyu

* Corresponding author (email: xuliubing@m.scnu.edu.cn)

Glaciations. Using cosmogenic radionuclide $^{10}$Be, Zhou et al. (2007, 2010) dated the Guxiang and Baiyu Glaciations to 136.5–112.9 and 18.5–11.1 ka, corresponding to marine oxygen isotope stage 6 (MIS-6) and stage 2 (MIS-2), respectively. Furthermore, the history of glacial fluctuations postdating the Last Glacial Maximum has been reconstructed based on numerical dating, confirming glacial advances during the Late Glacial, Neoglacial, and Little Ice Age (Jiao et al., 2005; Yang et al., 2005; Zhou et al., 2007, 2010; Ou et al., 2015; Chen et al., 2014, 2020; Hu et al., 2015, 2017). It has been demonstrated that glaciations predating MIS-6 occurred at many locations on the Tibetan Plateau and its surrounding mountains (Wang et al., 2006; Zhou et al., 2006; Xu and Zhou, 2009; Owen et al., 2010; Chen et al., 2018), posing the question: as a major glaciation center both at present and during the Quaternary, did a glaciation prior to MIS-6 ever occur in southeastern Tibet? During our recent field investigations, we identified a discontinuous lateral moraine lying on valley shoulders that are ~500–600 m above the Guxiang Glaciation moraine. Morphostratigraphically, this newly recognized moraine is definitely older than the Guxiang Glaciation. To constrain the timing of the associated glacier advance we applied electron spin resonance (ESR) to directly date the moraine deposits. Our finding is critical to better understand the whole history of Quaternary glacial fluctuations and tectonic uplift in southeastern Tibet.

## 2 Glaciological records

The Bodui Zangbo River, originating from the southern slope of the eastern Nyainqêntanglha Range, is a sub-tributary of the Yarlung Zangbo River (Figure 1). Zepu Kangri, the summit in the Bodui Zangbo catchment, has an elevation of 6364 m. In this catchment, there are 482 modern glaciers, covering a total area of about 974 km$^2$. The Zepu Glacier, having a length of 19.2 km and an area of 76.2 km$^2$, is the largest glacier in this area (Figure 2; Guo et al., 2014; Mi et al., 2002). The Zepu Glacier, together with other tributary glaciers, repeatedly advanced into and retreated from the Bodui Zangbo trunk valley, producing an ample record of past glaciations.

### 2.1 Glaciological evidence of Guxiang Glaciation

The wide Bodui Zangbo valley contains abundant well-preserved glacial and glaciofluvial landforms and sediments (Figure 2), among which the most extensive is the lateral moraine constructed during the Guxiang Glaciation. The moraine is largely continuously distributed along both sides of the Bodui Zangbo valley from Yuren Village to Baiyu Village, with the height (above the valley floor) decreasing from about 550 m at Yuren to approximately 260 m at Baiyu. In contrast, it is poorly preserved within the ~28 km down the valley from Baiyu, due to post-depositional fluvial and glacial erosion. However, a 3.2 km segment of the moraine, standing ~200 m above the valley floor, is well preserved at the Kada Bridge near the confluence of the Bodui Zangbo and Parlung Zangbo valleys (Figure 2). Apart from being extensively preserved in the Bodui Zangbo trunk valley, the Guxiang Glaciation moraine can also be traced in several tributaries (e.g., Yalong Zangbo valley), indicating an extensive dendritic valley glacier in the Bodui Zangbo drainage basin during the Guxiang Glaciation, with a length of over 100 km and a total area of 6–8 times of modern glaciers

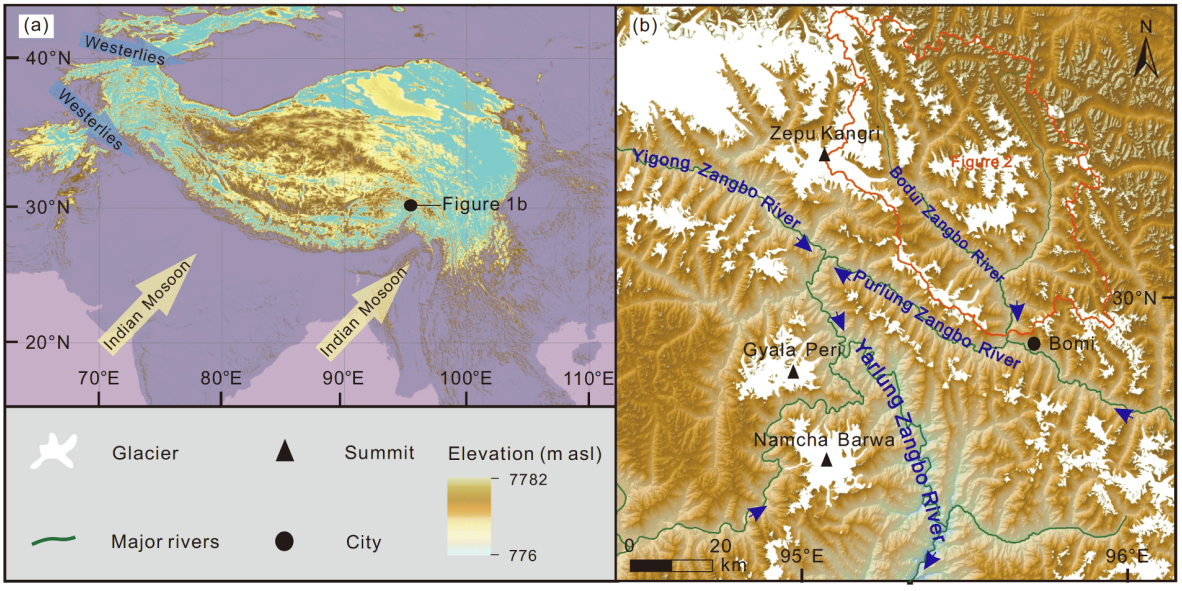


**Figure 1** Location of the study area (a) and its DEM (b). Major rivers, mountain peaks, and modern glaciers (white colored) are shown in (b).

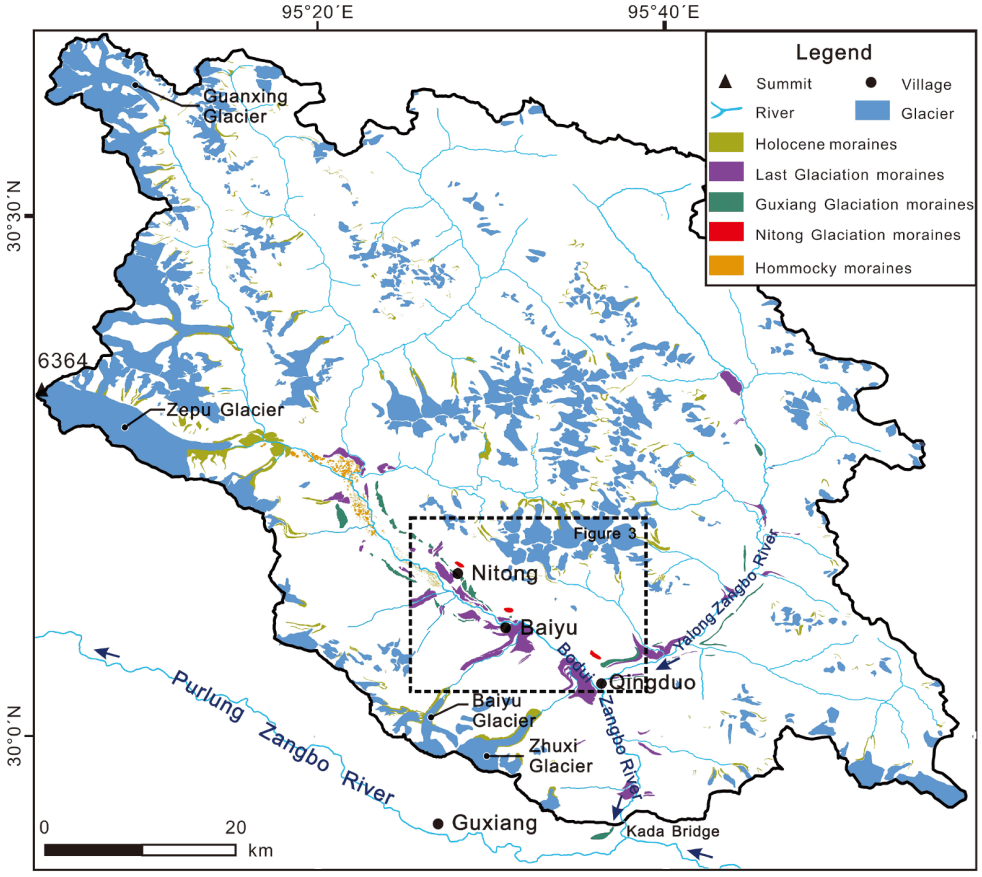


**Figure 2** Modern glaciers and glacial landforms of different glacial stages in the Bodui Zangbo catchment.

(Li et al., 1986). Zhou et al. (2007, 2010) dated the Guxiang Glaciation moraine at the Kada Bridge to ~130 ka (corresponding to MIS-6) using cosmogenic $^{10}$Be surface exposure dating.

## 2.2 Geomorphologic evidence for glacier advance prior to the Guxiang Glaciation

During our field investigations in the past several years, we identified a staircase of discontinuous valley shoulders along both sides of the Bodui Zangbo River valley, which are ~500–600 m above the Guxiang Glaciation moraine. Glacial deposits are relatively well preserved on some of the valley shoulder sites, for example, at Nitong, Baiyu, and Qingduo (Figures 3 and 4).

The glacial deposits at Nitong (30.16°N, 95.46°E; ~800 m above the Bodui Zangbo valley floor) lies on a valley shoulder which is about 530 m higher than the Guxiang Glaciation moraine (Figures 2, 3, 4 and 5a). The deposits still have a relatively well-preserved morainic morphology, although the outside reverse-slope has been a bit obscured by post-depositional surface processes such as slope deposition (Figure 5b). The moraine ridge has a length of ~200 m, stands about 8 m above the outside ground, and extends in a direction parallel to the Bodui Zangbo trunk valley, suggesting the moraine is likely a segment of a lateral moraine formed by the trunk glacier instead of adjacent tributary glaciers. Some granite boulders, varying in diameter from tens of centimeters to up to 4 m, are scattered on the moraine surface and most of them show deeply-weathered features. Compared to modern moraine ridges characterized by an inverted V shape, the cross profile of the Nitong moraine is relatively gentle (Figure 5b), indicating that it has undergone significant denudation.

On the valley shoulder opposite to Baiyu Village, there is a moraine remnant (30.13°N, 95.53°E), which is ~800 m above the valley floor and ~600 m higher than the Guxiang moraine (Figures 2, 3 and 5c). It has a length of ~250 m and approximately parallels to the trunk valley. Compared to that at Nitong, the residual moraine here has a less pronounced morainic morphology. The ridge of the moraine is relatively flat, with gullies flowing across the moraine top surface (Figure 5d), indicating considerable degradation of the moraine. A few deeply weathered granite boulders are scattered on the moraine surface, with their height less than 1 m and diameter of 1–2 m. In addition, limestone bedrock has been exposed in gullies on the inner side of the moraine, showing that the moraine (mainly comprising granite clasts

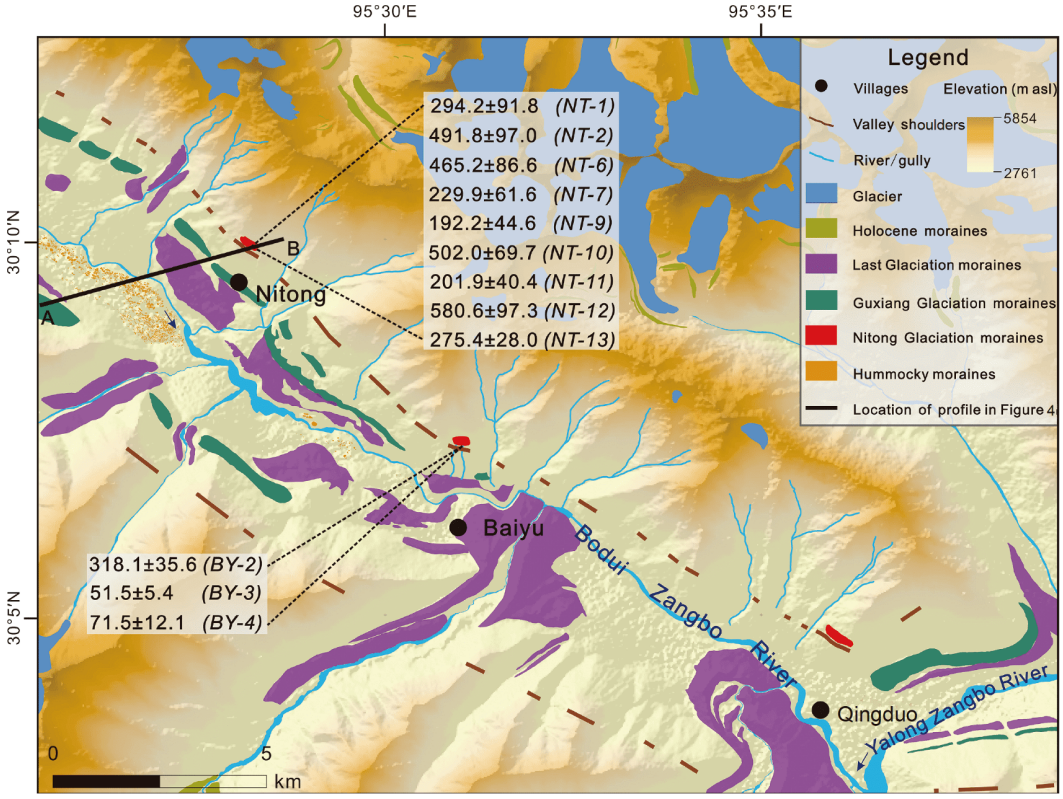


**Figure 3** Geomorphological map of the middle reach of the Bodui Zangbo valley, highlighting glacial landforms of different glacial stages, valley shoulders, ESR ages (unit: ka) of the Nitong Glaciation moraine, as well as the location of the profile in Figure 4.

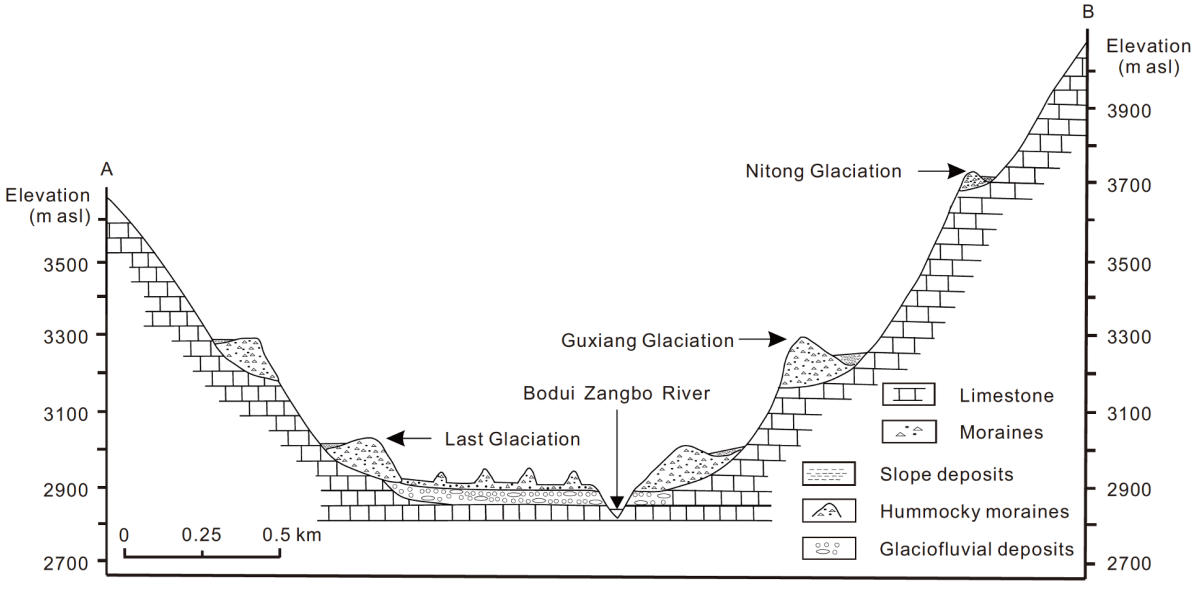


**Figure 4** Transverse profile across the Bodui Zangbo River valley near Nitong, highlighting the morphostratigraphic relationships of different phases of glacial landforms.

and blocks) could have not been constructed by adjacent tributary glaciers, but likely by the trunk glacier.

On the valley shoulder north to Qingduo, there is also a long area of glacial deposits (34.07°N, 95.55°E) (Figures 2 and 3), which are ~700 m above the valley floor and ~550 m higher than the Guxiang Glaciation moraine. There is not typical morainic morphology here. The deposits comprise a layer of deeply weathered clasts (1–2 m thick), with a few granite boulders (1–2 m in diameter) scattered on them.

The fact that all the moraines/glacial deposits at the three sites are basically parallel to the Bodui Zangbo trunk valley and are mainly composed of granite boulders and clasts,

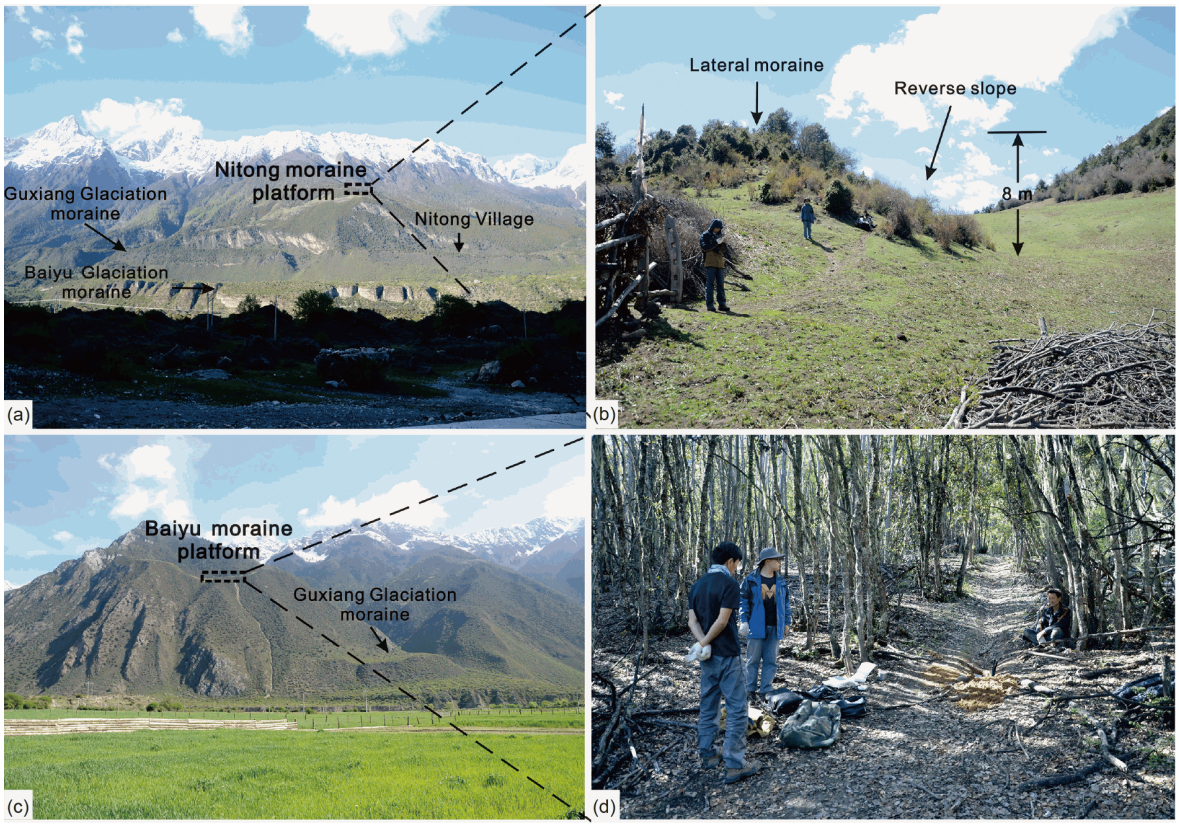


**Figure 5** Field photos of moraine segments at Nitong ((a), (b)) and Baiyu ((c), (d)).

suggests that they are likely formed by the trunk glacier rather than adjacent tributary glaciers. Furthermore, the moraines/deposits are located on valley shoulders of similar height (i.e., 700–800 m above the valley floor), indicating they could had been produced by the same glaciation. Considering all the moraines/deposits are ~500–600 m higher than the Guxiang Glaciation moraine, stratigraphically, they should have been formed prior to the Guxiang Glaciation. To our best knowledge, these glacial features are first reported in this area. Considering the morainic morphology of the glacial deposits at Nitong is the most typical among the three locations (Figures 4 and 5), here we temporarily name the glacial expansion forming the moraines/deposits as Nitong Glaciation. Below we will discuss the timing of the glaciation.

## 3 Methods

In the past decades, a variety of dating methods, for example, cosmogenic nuclide surface exposure dating, optically stimulated luminescence (OSL), electron spin resonance (ESR), and radiocarbon ($^{14}$C), have been widely used to constrain the timing of Quaternary glacial fluctuations. As mentioned above, the Nitong Glaciation should have occurred prior to the Guxiang Glaciation (MIS-6) based on their morphostratigraphic relationships. The gentle morphology of the Nitong Glaciation moraine also shows that it has experienced significant surface denudation. Despite that cosmogenic nuclide (particularly $^{10}$Be) surface exposure dating is currently the most frequently applied dating method in glacial chronology studies, it is not an appropriate method when the moraine to be dated has suffered dramatic erosion or denudation, because boulders on the moraine surface are likely exposed out from subsurface (Schaefer et al., 2008). In this case, the obtained exposure ages would underestimate the true age of the dated moraine. OSL (quartz single-aliquot regenerative-dose protocol) is also a commonly used method to constrain the timing of past glacial oscillations. However, as mentioned above, the Nitong Glaciation deposits should have been formed before MIS-6 and thus exceed the upper dating limit (typically 100–150 ka) of the method (Fuchs and Owen, 2008). What's more, a recent study shows that the annual dose rate in this region is relatively high, which would further shorten the upper dating limit (Ou et al., 2015). Due to the relatively low upper dating limit (<50 ka) and the lack of suitable dating material, $^{14}$C also cannot be applied to date the Nitong Glaciation. Therefore, ESR technique was chosen in this study. Experimental simulations (Gao et al., 2009; Liu and Grün, 2011; Yi et al., 2016) and case studies (Xu and

Zhou, 2009; Zhao et al., 2009a; Wang et al., 2019) have demonstrated that some ESR signals, for example, Al-, Ti-, Ge-, and $E_1'$-centers, can be applied to determine the burial age of quartz samples. In this study we choose the Ti-Li-center of Ti-centers (Figure 6) to directly date glacial deposits of the Nitong Glaciation.

As the glacial deposits at Qingduo are less well preserved, we only collected ESR dating samples from the Nitong and Baiyu moraine deposits, following conventional procedures as described in Liu et al. (2013) and Yi et al. (2019). Nine samples were collected from the Nitong moraine. Samples NT-6 and NT-12 were obtained at the moraine ridge; NT-1, NT-2, NT-7, NT-9, NT-10, NT-11, and NT-13 were sampled from the moraine slope, among which NT-2 and NT-10 are closer to the moraine crest than the other five samples. Samples NT-1 and NT-12 comprise grey-white, fine-grained sand and the rest seven samples consist of grey-brown, fine-grained sand (Figure 7). Three samples (BY-2, BY-3, and BY-4) were collected from a gully on the top of the Baiyu moraine. The sampling sections comprise dark yellow, silt- and fine-grained sand (Figure 7). Detailed information of all the samples is listed in Table 1.

Sample preparation was performed at the geochronology laboratory of South China Normal University. The samples were first soaked in dilute HCl and $H_2O_2$ to eliminate carbonate and organic matter, respectively. A strong magnet was used to remove magnetic minerals. The remaining particles were then dry-sieved to obtain the 120–200 μm fraction which were subsequently immersed into heavy liquid (sodium polytungstate) to separate quartz grains. The quartz grains were etched within 40% HF for about 80 min to remove feldspar, followed by 10% HCl to eliminate fluoride precipitates.

The pure quartz samples were irradiated using a $^{60}Co$ gamma source in Peking University, with a gamma dose rate of 28.51 Gy $min^{-1}$. The irradiated quartz grains were then measured on a BURKER ER041XG X-band spectrometer in the State Key Laboratory of Earthquake Dynamics, Institute of Geology, China Earthquake Administration. The measurement conditions are as follows: temperature: 77 K; X-band; microwave power: 5.1 mW; central field: 3400 G; sweep width: 320 G; microwave frequency: 9.468 GHz; modulation frequency: 100 kHz; modulation amplitude: 1 G; time constant: 40.96 ms; conversion time: 20.48 ms. A representative ESR spectrum is shown in Figure 6. Equivalent doses (De) were derived from exponentially fitting of the artificial irradiation doses and the corresponding ESR signal intensities (Figure 8).

The contents of U and Th were measured with an inductively coupled plasma mass spectrometry and $K_2O$ with a flame photometer, which were conducted in Beijing Research Institute of Uranium Geology. Annual dose rates were estimated from the contents of the radioactive elements (U, Th, and K), water contents, and cosmic ray contributions, following the method by Prescott and Hutton (1994). The measurement and calculated results are presented in Table 1.

## 4 Discussion

### 4.1 Reset mechanisms of Ti-centers in glacial quartz grains

ESR dating is based on the assumption that the ESR signals in mineral grains had been bleached when the sampled sediments were deposited. Previous studies have shown that manual grinding or exposure to sunlight could effectively

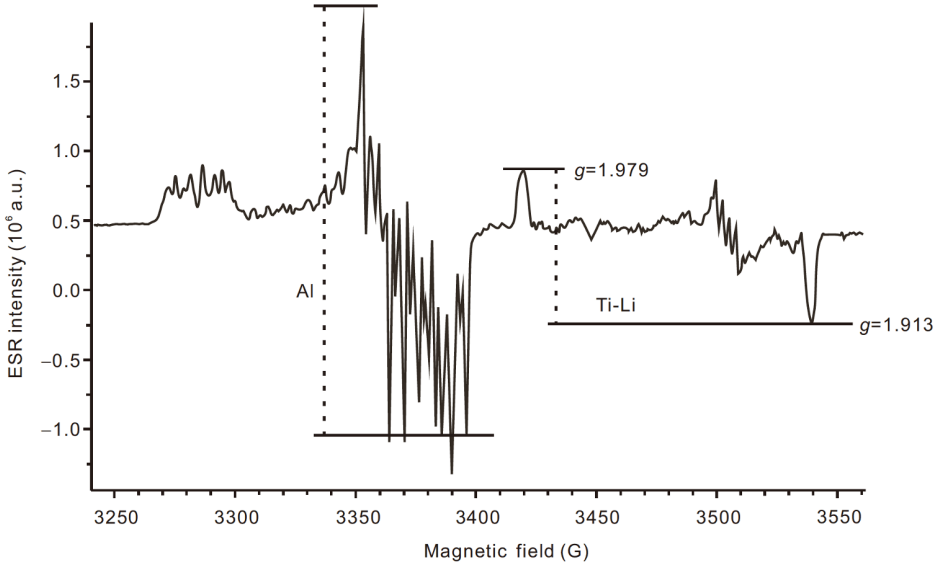


**Figure 6** ESR signal spectrums of Al- and Ti-Li-centers of sample NT-10 (additional radiation dose at 1600 Gy) under low temperature (liquid nitrogen, 77 K).


**Figure 7** Photos showing sampling sections.

bleach the ESR signals in sediments (Ye et al., 1998; Yi et al., 2016). Shear stress experiments showed that the ESR signal intensity of Ti-centers declines with the increase of stress, and that of finer quartz grains are more sensitive to stress than that of coarser grains (Buhay et al., 1988). The tumbler experiments by Liu and Grün (2011) indicated that mechanical collision could lead to a 37% reduction of the ESR intensity of Ti-centers in quartz grains from fluvial sediments and granite rocks. These experiments suggest that surface abrasion and mechanical crushing and collision between particles during their transportation, particularly under a high-pressure circumstance, are critical mechanisms for the weakening of ESR signals (Fukuchi et al., 1986; Lee and Schwarcz, 1993; Liu and Grün, 2011; Yi et al., 2016).

Optical exposure experiments suggested that the Ti-center ESR signals can be completely bleached after tens of hours of solar radiation (Rink et al., 2007; Yoshida, 2013). Bleaching experiments showed that the ESR signals of Ti-Li-centers in quartz grains can be fully zeroed after exposure to natural light for about 260 h (Wei et al., 2018). The signals of Ti-Li-centers can be totally bleached when samples are illuminated by simulated sunlight for 1–520 h (Tissoux et al., 2007; Liu et al., 2013). In contrast, the time required to fully reset the ESR signals is only 15 min when samples are irradiated using a UV lamplight (Tanaka et al., 1997). It took 64 and 56 h to reset the ESR signals of Ti-Li-centers when samples were exposed to sunlight at Germu (2760 m asl) and Lhasa (3600 m asl), respectively (Gao et al., 2009), indicating that the time required for the resetting of the Ti-Li-center ESR signals varies inversely with the intensity of ultraviolet rays or with the elevations of samples.

A lateral moraine is typically formed by the dumping of superglacially melt-out tills at ice margins (Cui et al., 1981; Benn and Owen, 2002). During this process, the tills could have enough time to be exposed to sunlight and thus are likely to be bleached (Yi et al., 2016, 2019). In addition, part of englacial and subglacial tills may be transported onto ice surface. These tills are more likely to be bleached because they are squeezed out through shear planes under huge shear stress.

As mentioned above, the Bodui Zangbo valley was occupied by a large-size temperate glacier during the Nitong

**Table 1** Sample information and ESR dating results[a)]

| Sample number | Sample information | | | | U ($\mu g\ g^{-1}$) | Th ($\mu g\ g^{-1}$) | $K_2O$ (%) | Water content (%)[a)] | Cosmic (mGy $a^{-1}$) | De (Gy) | Age (ka) |
|---|---|---|---|---|---|---|---|---|---|---|---|
| | Longitude Latitude | Altitude (m) | Location | Depth (m) | | | | | | | |
| NT-1 | 30.167638°N 95.469306°E | 3775 | Nitong moraine slope | 0.5 | 1.98 | 12.7 | 1.8 | 3 | 0.3435 | 1029.73±319.38 | 294.2±91.8 |
| NT-2 | 30.165222°N 95.469389°E | 3760 | Near Nitong moraine ridge | 0.8 | 1.94 | 14.2 | 1.9 | 3 | 0.3424 | 1762.28±342.05 | 491.8±97.0 |
| NT-6 | 30.165830°N 95.469250°E | 3765 | Nitong moraine ridge | 1.0 | 2.58 | 17.3 | 1.7 | 15.1 | 0.3429 | 1672.08±306.43 | 465.2±86.6 |
| NT-7 | 30.165580°N 95.469610°E | 3757 | Nitong moraine slope | 0.5 | 1.85 | 17.1 | 1.4 | 16.2 | 0.3424 | 753.59±200.60 | 229.9±61.6 |
| NT-9 | 30.165560°N 95.469670°E | 3757 | Nitong moraine slope | 0.8 | 2.56 | 26.7 | 2.1 | 8.2 | 0.3424 | 772.85±177.32 | 192.2±44.6 |
| NT-10 | 30.165690°N 95.469610°E | 3760 | Near Nitong moraine ridge | 1.0 | 2.3 | 21.4 | 1.6 | 19.7 | 0.3425 | 1801.57±243.23 | 502.0±69.7 |
| NT-11 | 30.165500°N 95.469310°E | 3755 | Nitong moraine slope | 0.8 | 2.74 | 24.8 | 2 | 30.9 | 0.3422 | 792.60±156.30 | 201.9±40.4 |
| NT-12 | 30.165330°N 95.469310°E | 3759 | Nitong moraine ridge | 0.8 | 2.37 | 22.7 | 1.7 | 14.3 | 0.3419 | 2138.92±351.43 | 580.6±97.3 |
| NT-13 | 30.165390°N 95.469500°E | 3751 | Nitong moraine slope | 0.5 | 2.13 | 20 | 1.8 | 16.5 | 0.3420 | 1013.72±97.10 | 275.4±28.0 |
| BY-2 | 30.122917°N 95.530556°E | 3496 | top of Baiyu moraine | 1.0 | 1.9 | 22.1 | 2.2 | 4.7 | 0.3260 | 1277.90±135.60 | 318.1±35.6 |
| BY-3 | 30.120833°N 95.517222°E | 3463 | top of Baiyu moraine | 0.5 | 3.55 | 24.6 | 2.2 | 2.5 | 0.3240 | 213.03±21.13 | 51.5±5.4 |
| BY-4 | 30.120833°N 95.517222°E | 3463 | top of Baiyu moraine | 0.5 | 2.91 | 24.6 | 2.2 | 2.5 | 0.3240 | 291.32±48.10 | 71.5±12.1 |

a) Water contents were assumed to be (10±5)%.

Glaciation. According to modern observations, such a glacier is generally characterized by a high ice-flow velocity and intense englacial abrasion and crushing, which could produce abundant, highly bleached fine grains. Furthermore, our sampling sites are as far as 70 km from the source area, which allows superglacial tills to be exposed to sunlight for enough time. Taking these together, we suggest that the Ti-Li-center ESR signals of our 12 samples, comprised of fine sand and/or silt, are likely to be zeroed prior to deposition.

### 4.2 Dating results

For the moraine segment at Nitong, samples NT-2, NT-6, NT-10, and NT-12, collected from the top area of the moraine, produce ESR ages ranging from 581 to 465 ka, whereas the rest five samples (NT-1, NT-7, NT-9, NT-11 and NT-13), which were obtained from near the toe of the moraine slope, yield much younger ages, varying from 294 to 192 ka (Table 1). Morainic morphology studies show that a newly constructed moraine typically has a slope of around 34° (Putkonen and Swanson, 2003). However, the Nitong moraine is characterized by a quite subdued shape and the slope is less than 10° (Figure 5b), suggesting the moraine has suffered considerable denudation. Simulations of topographic evolution of moraines show that, as time goes on, material at the moraine crest is gradually transported to the toe of the moraine slope and resultantly, the moraine becomes much gentler than its original sharp-crested shape (Figure 9; Hallet and Putkonen, 1994; Applegate et al., 2010). This means the ESR ages of the samples taken from the top (erosional area) of the moraine likely represent the true deposition time of the moraine although it has experienced significant erosion; in contrast, the sample ages from the toe of the moraine slope (depositional area) are expected to reflect the time when the sampled sediments were redeposited (Figure 9). Following this hypothesis, we consider it most likely that the ages of the four samples (NT-2, NT-6, NT-10, and NT-12) from the moraine top area reflect the real deposition time of the Nitong moraine, but considering the ESR signal of sample NT-10 is almost saturated (Figure 8), the age of NT-10 will be excluded from further consideration. In contrast, the other five ages (NT-1, NT-7, NT-9, NT-11, NT-13) from the lower part of the moraine slope likely underestimate the deposition time of the moraine; particularly, the ESR signals of three (NT-7, NT-9, and NT-11) of them are (nearly) saturated. We therefore consider the five samples (NT-1, NT-7, NT-9, NT-11, NT-13) as outliers and exclude them from further discussion.

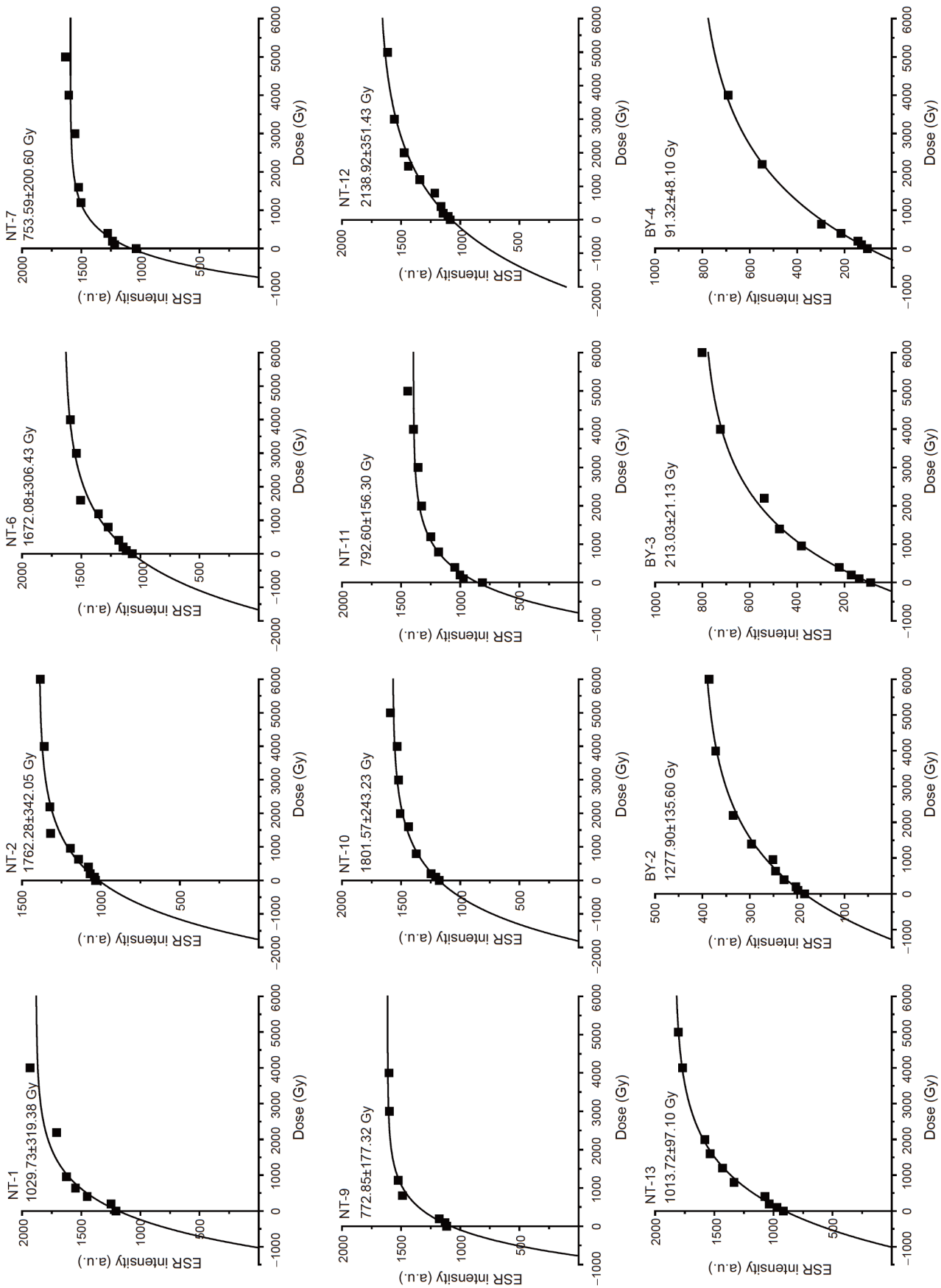


**Figure 8** Fitting curves between artificial radiation doses and ESR signal intensities.

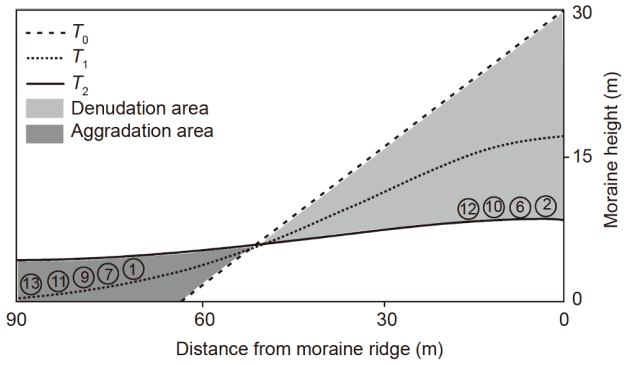


**Figure 9** Evolution process of the moraine at Nitong with time. Numbers indicate relative positions of samples; lines show profiles of the moraine at different times.

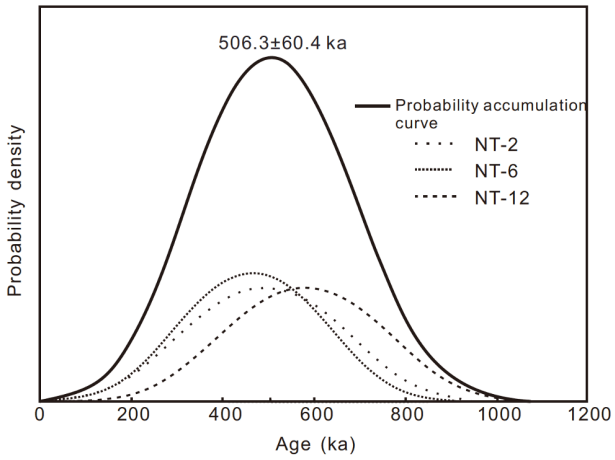


**Figure 10** Normal kernel density estimate of the age for the moraine at Nitong. Thick black line represents summed probability of individual age probabilities (dashed lines).

For the moraine residual at Baiyu, samples BY-2, BY-3, and BY-4 have ages of about 320, 50, and 70 ka, respectively. These ESR ages are significantly younger than those obtained from the top area of the moraine at Nitong. As mentioned above, these three samples were collected from a gully on the top of the moraine, we thus speculate the samples might have been reworked or disturbed by gully erosion. Consequently, these ages cannot represent the deposition time of the moraine and will be excluded in the following discussion.

In summary, we suggest that three (NT-2, NT-6, and NT-12) of the 12 ESR ages likely provide the best estimate of the timing of the Nitong Glaciation. The three ages range from 580.6±97.3 to 465.2±86.6 ka. By using a normal kernel density function, we get a peak value of 506.3±60.4 ka ($1\sigma$ uncertainty) (Figure 10), corresponding to MIS-14–12. Taking into account the age error and climatic conditions, it is most likely that the Nitong Glaciation occurred during MIS-12, although we cannot exclude the possibility that the glacial expansion occurred during MIS-14 or even earlier.

### 4.3 Background for the Nitong Glaciation

The commencement of glaciation on the Tibetan Plateau is far later than that in both polar regions. It has been suggested that glaciation on the plateau is resulted from the combination of surface uplift and glacial climate, that is, glaciation would not occur until the plateau had been uplifted above the climatic snow line during a glacial period (Zhou and Li, 2003; Zhou et al., 2006; Chen et al., 2019). It was until the Kunlun-Huanghe tectonic movement (~1.1–0.6 Ma) that the Tibetan Plateau had been entirely uplifted to the elevation of 3000–3500 m (Cui et al., 1998). Almost simultaneously, the global temperature decreased notably during the Middle Pleistocene transition (Head and Gibbard, 2005). The coupling of these two factors led to the earliest glaciation on the Tibetan Plateau (Zhou and Li, 2001; Chen et al., 2018). However, due to the spatial diversity of uplift amplitude and climatic conditions on the broad plateau (Jiang et al., 2019), the timing of initial glaciation varies significantly from mountain to mountain (Zheng et al., 2002). For example, the Shishapangma Glaciation, the earliest glaciation in the Himalayas, likely occurred around MIS-20 (Chen et al., 2018). The onset of glaciation in the Hengduan Mountains and western Nyainqêntanglha Range probably took place during MIS-18–16 (Zhou et al., 2005; Wang et al., 2006; Xu and Zhou, 2009).

Sedimentary evidence from the eastern Nyainqêntanglha Range shows that the mountain experienced intense tectonic uplift during the Early Pleistocene (Zhu et al., 2002). $\delta^{18}O$ records from deep-sea cores suggest that MIS-12 is one of the periods when the continents were most extensively glaciated (Lisiecki and Raymo, 2005). Climate proxy records from RH and RM cores in the Rouergai Basin on the eastern Tibetan Plateau also indicate that the climate was extremely cold during MIS-12 (Wang et al., 1994). It is likely that the coupling of these two critical drivers (namely, surface uplift and decreased temperatures) caused the extensive glacier advance during the Nitong Glaciation in the eastern Nyainqêntanglha Range. Glacial expansions during MIS-12 have also been verified in many other regions on the Tibetan Plateau as well as in the surrounding mountains. For example, the Naimon'anyi Glaciation on the Naimon'anyi massif in the western Himalaya was dated to 491–423 ka (Owen et al., 2010; recalculated cosmogenic $^{10}$Be exposure ages based on the latest $^{10}$Be production rate and scaling model). In the Qilian Mountains, the Zhonglianggan Glaciation in the Bailang River area was dated to ~463 ka (Zhou et al., 2001a). In the Tianshan Mountains, the MIS-12 glaciation has been identified at least at three locations, the High Wangfeng Glaciation in the Urumqi River valley (Zhou et al., 2001b), the Qingshantou Glaciation in the Ateaoyinake River catchment (Zhao et al., 2009a), and the oldest glacia-

tion of in the Tumur River valley (Zhao et al., 2009b). In the Hengduan Mountains, evidence has been reported for the MIS-12 glacial expansion in the Yulong and Baima Snow Mountains, as well as in the Luoji Mountain (Zhao et al., 1999; Zhang et al., 2015; 2017).

## 5 Conclusions

Morphostratigraphic evidence suggests a glacial expansion prior to the Guxiang Glaciation (MIS-6) in the Bodui Zangbo River valley in the eastern Nyainqêntanglha Range, southeastern Tibet. Here we name the glacial expansion as Nitong Glaciation. Using the ESR method, we dated the lateral moraine deposits of the Nitong Glaciation to 506.3±60.4 ka. Taking into account the age error and climatic conditions, it is most likely that the Nitong Glaciation occurred during MIS-12, although it might occur sometime earlier. Our finding is critical to better understand the whole history of Quaternary glacial fluctuations and tectonic uplift in southeastern Tibet.

**Acknowledgements** *This work was supported by the National Natural Science Foundation of China (Grant Nos. 41771065, 42071088, 41271077 and 41371080). We thank Professors Jianping Li and Chunru Liu from the State Key Laboratory of Earthquake Dynamics, Institute of Geology, China Earthquake Administration, for their assistance in the ESR experiments. We are also grateful to two anonymous reviewers for their constructive comments that helped to significantly improve the quality of the manuscript.*

## References

Applegate P J, Urban N M, Laabs B J C, Keller K, Alley R B. 2010. Modeling the statistical distributions of cosmogenic exposure dates from moraines. Geosci Model Dev, 3: 293–307

Benn D I, Owen L A. 2002. Himalayan glacial sedimentary environments: A framework for reconstructing and dating the former extent of glaciers in high mountains. Quat Int, 97-98: 3–25

Buhay W M, Schwarcz H P, Grün R. 1988. ESR dating of fault gouge: The effect of grain size. Quat Sci Rev, 7: 515–522

Chen F H, Fu B J, Xia J, Wu D, Wu S H, Zhang Y L, Sun H, Liu Y, Fang X M, Qin B Q, Li X, Zhang T J, Liu B Y, Dong Z B, Hou S G, Tian L D, Xu B Q, Dong G H, Zheng J Y, Yang W, Wang X, Li Z J, Wang F, Hu Z B, Wang J, Liu J B, Chen J H, Huang W, Hou J Z, Cai Q F, Long H, Jiang M, Hu Y X, Feng X M, Mo X G, Yang X Y, Zhang D J, Wang X H, Yin Y H, Liu X C. 2019. Major advances in studies of the physical geography and living environment of China during the past 70 years and future prospects. Sci China Earth Sci, 62: 1665–1701

Chen R R, Zhou S Z, Lai Z P, Ou X J, Chen R, Deng Y B. 2014. Luminescence chronology of late Quaternary moraines and Last Glacial Maximum equilibrium-line altitude reconstruction from Parlung Zangbo Valley, south-eastern Tibetan Plateau. J Quat Sci, 29: 597–604

Chen R R, Zhou S Z, Li Y K, Lai Z P, Ou X J, Lu X, Li Y N. 2020. Late Quaternary climate and environmental change derived from glacial deposits in the Parlung Zangbo Valley, southeastern Tibetan Plateau. Phys Geogr, 41: 99–125

Chen Y X, Li Y K, Zhang M, Cui Z J, Liu G N. 2018. Much late onset of Quaternary glaciations on the Tibetan Plateau: Determining the age of the Shishapangma Glaciation using cosmogenic $^{26}$Al and $^{10}$Be dating. Sci Bull, 63: 306–313

Cui Z J, Ren B H, Li J J. 1981. On the conception and translation of terms of glacial tills (in Chinese). J Glaciol Geochryol, 3: 78–82

Cui Z J, Wu Y Q, Liu G N, Ge D K, Pang Q Q, Xu Q H. 1998. On Kunlun-Yellow river tectonic movement. Sci China Ser D-Earth Sci, 41: 592–600

Fuchs M, Owen L A. 2008. Luminescence dating of glacial and associated sediments: Review, recommendations and future directions. Boreas, 37: 636–659

Fukuchi T, Imai N, Shimokawa K. 1986. ESR dating of fault movement using various defect centres in quartz: The case in the western South Fossa Magna, Japan. Earth Planet Sci Lett, 78: 121–128

Gao L, Yin G M, Liu C R, Bahain J J, Lin M, Li J P. 2009. Natural sunlight bleaching of the ESR titanium center in quartz. Radiat Meas, 44: 501–504

Guo W Q, Xu J L, Liu S Y, Shangguan D H, Wu L Z, Yao X J, Zhao J D, Liu Q, Jiang Z L, Li Ping, Wei J F, Bao W J, Yu P C, Ding L F, Li G, Gai C M, Wang Y. 2014. The Second Glacier Inventory Dataset of China (Version 1.0) (in Chinese). Lanzhou: Cold and Arid Regions Science Data Center

Hallet B, Putkonen J. 1994. Surface dating of dynamic landforms: Young boulders on aging moraines. Science, 265: 937–940

Head M J, Gibbard P L. 2005. Early-Middle Pleistocene transitions: An overview and recommendation for the defining boundary. Geol Soc London Spec Publ, 247: 1–18

Hu G, Yi C L, Zhang J F, Dong G C, Liu J H, Xu X K, Jiang T. 2017. Extensive glacial advances during the Last Glacial Maximum near the eastern Himalayan syntaxis. Quat Int, 443: 1–12

Hu G, Yi C L, Zhang J F, Liu J H, Jiang T. 2015. Luminescence dating of glacial deposits near the eastern Himalayan syntaxis using different grain-size fractions. Quat Sci Rev, 124: 124–144

Jiang D B, Liu Y Y, Lang X M. 2019. A multi-model analysis of glacier equilibrium line altitudes in western China during the last glacial maximum. Sci China Earth Sci, 62: 1241–1255

Jiao K Q, Iwata S, Yao T D, Jing Z F, Li Z Q. 2005. Variation of Zepu Glacier and environmental change in the eastern Nyainqentanglha range since 3.2 ka BP (in Chinese). J Glaciol Geochryol, 27:74–79

Lee H K, Schwarcz E P. 1993. An experimental study of shear-induced zeroing of ESR signals in quartz. Appl Radiat Isotopes, 44: 191–195

Li J J, Zheng B X, Yang X J. Xie Y Q, Zhang L Y, Ma Z M, Xu S Y. 1986. Glaciers in Tibet (in Chinese). Beijing: Science Press

Lisiecki L E, Raymo M E. 2005. A Pliocene-Pleistocene stack of 57 globally distributed benthic $\delta^{18}$O records. Paleoceanography, 20: PA1003

Liu C R, Grün R. 2011. Fluvio-mechanical resetting of the Al and Ti centres in quartz. Radiat Meas, 46: 1038–1042

Liu C R, Yin G M, Zhang H P, Zheng W J, Voinchet P, Han F, Wang D, Song W J, Bahain J J. 2013. ESR geochronology of the Minjiang River terraces at Wenchuan, eastern margin of Tibetan Plateau, China. Geochronometria, 40: 360–367

Mi D S, Xie Z C, Luo X R. 2002. Glacier Inventory of China of the Ganga Drainage Basin and the River Drainage Basin (in Chinese). Xi'an: Xi'an Cartographic Publishing House

Ou X J, Duller G A T, Roberts H M, Zhou S Z, Lai Z P, Chen R, Chen R R, Zeng L H. 2015. Single grain optically stimulated luminescence dating of glacial sediments from the Baiyu Valley, southeastern Tibet. Quat Geochronol, 30: 314–319

Owen L A, Yi C L, Finkel R C, Davis N K. 2010. Quaternary glaciation of Gurla Mandhata (Naimon'anyi). Quat Sci Rev, 29: 1817–1830

Prescott J R, Hutton J T. 1994. Cosmic ray contributions to dose rates for luminescence and ESR dating: Large depths and long-term time variations. Radiat Meas, 23: 497–500

Putkonen J, Swanson T. 2003. Accuracy of cosmogenic ages for moraines. Quat Res, 59: 255–261

Rink W J, Bartoll J, Schwarcz H P, Shane P, Bar-Yosef O. 2007. Testing the reliability of ESR dating of optically exposed buried quartz sediments. Radiat Meas, 42: 1618–1626

Schaefer J M, Oberholzer P, Zhao Z, Ivy-Ochs S, Wieler R, Baur H, Kubik

P W, Schlüchter C. 2008. Cosmogenic beryllium-10 and neon-21 dating of late Pleistocene glaciations in Nyalam, monsoonal Himalayas. Quat Sci Rev, 27: 295–311
Tanaka K, Hataya R, Spooner N A, Questiaux D G, Saito Y, Hashimoto T. 1997. Dating of marine terrace sediments by ESR, TL and OSL methods and their applicabilities. Quat Sci Rev, 16: 257–264
Tissoux H, Falguères C, Voinchet P, Toyoda S, Bahain J J, Despriée J. 2007. Potential use of Ti-center in ESR dating of fluvial sediment. Quat Geochronol, 2: 367–372
Wang G, Feng Z G, Gu J N, Zhao Z Z. 2019. Quaternary glaciation remains and glaciation sequences around the Kunlun Pass (in Chinese). J Glaciol Geochryol, 41: 64–74
Wang S M, Shi Y F, Shen J. 1994. Preliminary study on the plaleoclimate and paleoenvironment evolution of the east of Qinghai-Xizang Plateau since 800 ka BP (in Chinese). In: Sun H L, Zheng D, Liu D S, Shi Y F, Li J J, Zhang X S, Li W H, Pan Y S, Kong X R, Tang M C, Lu Y Z, eds. Study on the Formation Evolution, Environment Change and Ecosystem of the Qinghai-Xizang Plateau. Beijing: Science Press. 236–248
Wang J, Raisbeck G, Xu X B, Yiou F, Bai S B. 2006. *In situ* cosmogenic $^{10}$Be dating of the Quaternary glaciations in the southern Shaluli Mountain on the Southeastern Tibetan Plateau. Sci China Ser D-Earth Sci, 49: 1291–1298
Wei C Y, Liu C R, Li C A, Leng Y H, Li W P, Yin G M, Han F, Li J P. 2018. Bleaching characteristics of quartz electron spin resonance (ESR) signals of multiple Ti-Li centers: Implication for ESR dating (in Chinese). J Earth Environ, 9: 607–613
Xu L B, Zhou S Z. 2009. Quaternary glaciations recorded by glacial and fluvial landforms in the Shaluli Mountains, Southeastern Tibetan Plateau. Geomorphology, 103: 268–275
Yang W, Zhou S Z, Wang J, Wang X L, Sun A Z, Xu L B, Han H T. 2005. Formation mechanism of hummocky moraine in the Bodui Zangbo Valley and its environmental significance (in Chinese). J Glaciol Geochryol, 27: 220–225
Ye Y G, Diao S B, He J, Gao J C, Lei X Y. 1998. ESR dating studies of palaeo-debris-flow deposits in Dongchuan, Yunnan Province, China. Quat Sci Rev, 17: 1073–1076
Yi C L, Bi W L, Li J P. 2016. ESR dating of glacial moraine deposits: Some insights about the resetting of the germanium (Ge) signal measured in quartz. Quat Geochronol, 35: 69–76
Yi C L, Bi W L, Yang H J. 2019. Genesis types of glacial sediments and sampling procedures for ESR dating (in Chinese). Geol Rev, 65: 1–17
Yoshida H. 2013. Quaternary dating studies using ESR signals, with emphasis on shell, coral, tooth enamel and quartz. Dissertation for Doctoral Degree. Canberra: Australian National University
Zhang W, Bi W L, Liu B B, Liu X, Zhang B, Li C. 2015. Geochronology constrainted on late Quaternary glaciation of Baimaxue Shan (in Chinese). Quat Sci, 35: 20–37
Zhang W, Liu L, Chai L, He D W. 2017. Characteristics of Quaternary glaciations using ESR dating method in the Luoji Mountain, Sichuan Province (in Chinese). Quat Sci, 32: 281–292
Zhao J D, Liu S Y, He Y Q, Song Y G. 2009a. Quaternary glacial chronology of the Ateaoyinake River valley, Tianshan mountains, China. Geomorphology, 103: 276–284
Zhao J D, Wang J, Shangguan D H. 2009b. Sequences of the Quaternary glacial sediments and their preliminary chronology in the Tumur River valley, Tianshan Mountains (in Chinese). J Glaciol Geochryol, 31: 628–633
Zhao X T, Qu Y X, Li T S. 1999. Pleistocene Glaciations along the eastern foot of the Yulong Mountains (in Chinese). J Glaciol Geochryol, 21: 242–248
Zheng B X, Xu Q, Shen Y. 2002. The relationship between climate change and Quaternary glacial cycles on the Qinghai-Tibetan Plateau: Review and speculation. Quat Int, 97-98: 93–101
Zhou S Z, Li J J. 2001. Advance of study on Qinghai-Xizang Plateau in ice ages (in Chinese). Earth Sci Front, 8: 67–76
Zhou S Z, Li J J. 2003. New dating results of Quaternary Glaciations in China (in Chinese). J Glaciol Geochryol, 25: 660–666
Zhou S Z, Li J J, Zhang S Q, Zhao J D. 2001a. Glacial geomorphology and ice ages in the Bailang River Basin, Qilian Mountains (in Chinese). J Glaciol Geochryol, 23: 131–138
Zhou S Z, Wang J, Xu L B, Wang X L, Colgan P M, Mickelson D M. 2010. Glacial advances in southeastern Tibet during late Quaternary and their implications for climatic changes. Quat Int, 218: 58–66
Zhou S Z, Wang X L, Wang J, Xu L B. 2006. A preliminary study on timing of the oldest Pleistocene glaciation in Qinghai-Tibetan Plateau. Quat Int, 154-155: 44–51
Zhou S Z, Xu L B, Cui J X, Zhang X W, Zhao J D. 2005. Geomorphologic evolution and environmental changes in the Shaluli Mountain region during the Quaternary. Chin Sci Bull, 50: 52–57
Zhou S Z, Xu L B, Colgan P M, Mickelson D M, Wang X L, Wang J, Zhong W. 2007. Cosmogenic $^{10}$Be dating of Guxiang and Baiyu glaciations. Chin Sci Bull, 52: 1387–1393
Zhou S Z, Yi C L, Shi Y F, Ye Y G. 2001b. Study on the ice age MIS-12 in western China (in Chinese). J Glaciol Geochryol, 7: 321–327
Zhu D G, Zhao X T, Meng X G, Wu Z H, Shao Z G, Feng X Y, Wang J, Yang C B. 2002. Fabric analysis of gravel in Quaternary gravel beds on backbone area of Niqingtanggulashan Mountains (in Chinese). J Geomech, 8: 323–332

(Responsible editor: Ninglian WANG)